

Denaturation bubbles in fluctuating DNA chains

J. PALMERI, M. MANGHI and N. DESTAINVILLE

Laboratoire de Physique Théorique, Université Paul Sabatier, CNRS; 118 route de Narbonne, 31062 Toulouse, France

PACS. 87.10.+e – General theory and mathematical aspects.

PACS. 87.15.Ya – Fluctuations.

PACS. 82.39.Pj – Nucleic acids, DNA and RNA bases.

Abstract. – A statistical model of DNA, coupling base pair states (unbroken or broken) and thermal chain fluctuations, is formulated and then investigated using an exact solution obtained by transfer kernel techniques. The dependence on temperature and DNA length of the fraction of denaturation bubbles and their correlation length are deduced. Novel results include (i) the melting temperature emerges naturally as a function of double-strand and bubble bending rigidities and (ii) mechanical and statistical properties of DNA, such as persistence length and mean square radius, are explicitly calculated on the same footing as base pair quantities.

Introduction. – The stability of double-stranded DNA (dsDNA) at physiological temperature is due to self-assembly: of base pairs within a same strand *via* base-stacking interactions between neighboring bases and of both strands *via* hydrogen bonds between pairs of complementary bases. The interaction between each complementary base pair is, however, on the order of $k_B T$ [1,2] (thermal energy) and thus thermal fluctuations can lead, even at physiological temperature, to local and transitory unzipping of the double strand [3,4]. The cooperative opening of several consecutive base pairs leads to denaturation bubbles which are likely to play a role from a biological perspective, since they may interfere with mechanisms such as replication, transcription or protein binding. For example, it has been proposed [5] that *transcription start sites* and *regulatory sites* could be related to DNA regions which have a higher probability of promoting bubbles. Indeed, the energy needed to break an adenine-thymine (A-T) base pair, connected by two hydrogen bonds, is smaller than the energy needed to break a guanine-cytosine (G-C) one (3 hydrogen bonds) [1]. At the same temperature, A-T rich sequences present *a priori* more bubbles than G-C rich ones, even though sequence effects on the occurrence of bubbles are more complex than a simple examination of local A-T base abundance [1,5]. In addition to the sequence, the fraction of denaturation bubbles naturally depends on temperature, as well as on the ionic strength of the solution [3]. In particular, the melting temperature above which DNA is completely denatured into two single-strand DNA (ssDNA) chains depends on both sequence and ionic strength. More intriguingly, another parameter that affects the melting temperature is the length of the double strand [6]. This is not a purely academic debate because short DNA strands (a few tens of base pairs) are involved in DNA chip experiments where the hybridization process is precisely affected by temperature in a way depending on strand length and sequence [7].

Another physical property of DNA that is influenced by the presence of denaturation bubbles is its bending rigidity because ssDNA is two orders of magnitude more flexible than dsDNA at normal salt concentration. Denaturation bubbles are therefore supposed to facilitate bending of the otherwise rigid polymer DNA in structures where it coils up with curvature radii down to 10 nm (despite a persistence length equal to 50 nm) in such situations as cyclization, loop formation, or packaging of DNA into nucleosomes [8]. The current rapid development of force experiments in magnetic or optical tweezer traps [9], “Tethered Particle Motion” experiments [10] or even more recently atomic force microscopy ones [11], is also a formidable opportunity to investigate directly the elastic properties of DNA strands as a function of length, temperature and salt concentration.

Microscopic models have been proposed to account for the thermodynamical properties of denaturation bubbles in DNA. They range from Ising-like two-state models, where the base pairs can be open or closed [6], to more sophisticated ones where the shape of the interaction potential between base pairs is more precisely taken into account [12]. When the bending rigidity is introduced in these models, however, its coupling with the previously introduced internal degrees of freedom is not explicitly written in the free energy of the model. It is always taken into account as an effect that renormalizes the parameters of the bare model, but in a way that is estimated *a priori* [6]. The model proposed here incorporates precisely this dependence of the polymer bending rigidity on the state of base pairs. It couples explicitly an Ising model, describing the internal degrees of freedom (open or closed), and a Heisenberg model, accounting for the rotational degrees of freedom between successive monomers of the DNA chain. Its originality lies in the fact that the internal 2-state and external bending degrees of freedom are treated on an equal footing and therefore the renormalized Ising parameters can be exactly calculated within the scope of the model. The melting temperature T_m naturally emerges in this coupled model and, together with the transition width, are explicitly written as a function of the bending rigidities and the strand length. In addition, the effective Ising properties (fraction of broken bases, correlation length) as well as the chain ones (persistence length, mean square radius) can be computed, allowing in principle direct comparison with experiment. An important feature of this effective Ising model is that the end monomers have a higher probability of remaining in the closed state leading to a chain length dependence of the transition temperature and width, and correlation functions. This exactly solvable model had been previously proposed by one of us [13], but its application to the study of denaturation bubbles in dsDNA was not made explicit. Recently, a similar model has been considered in the context of the dsDNA B to S-form stretching transition [14]. The addition in the energy functional of the term corresponding to the external force breaks rotational symmetry and prevents an exact solution of the model in [14]. Beyond dsDNA or dsRNA, our coupled Ising-chain model intends to describe the properties of any two-state biopolymer, as soon as the local bending rigidity depends on the local state. For example, the helix-coil transition in polypeptides can be described by such a model because the α -helix configuration is much more rigid than the random one [6].

Effective Ising model. – We model dsDNA as a discrete chain of N monomers (links), where each monomer can be in one of two different states, A and B (unbroken and broken bonds). The state of link i is denoted by the value of an Ising variable $\sigma_i = \pm 1$ (A or B). The local chain rigidity depends on the nearby link types. The chain’s conformational properties are determined by the set of N unit link tangent vectors $\mathbf{t}_i \{i = 1, \dots, N\}$. For simplicity, the monomer length, a , is taken to be the same for both A and B. The end-to-end vector is $\mathbf{R} = a \sum_{i=1}^N \mathbf{t}_i$. Up to an absolute location in space a state of the chain is given by the $2N$ variables $\{\sigma_i, \mathbf{t}_i\}$. Each link vector can be expressed in spherical coordinates as

$\mathbf{t}_i = (\sin(\theta_i) \cos(\phi_i), \sin(\theta_i) \sin(\phi_i), \cos(\theta_i))$ and can therefore be denoted by the solid angle $\Omega_i = (\theta_i, \phi_i)$. The energy $H[\sigma_i, \mathbf{t}_i]$ of a state is taken to be ($\beta = k_B T^{-1}$)

$$\beta H[\sigma_i, \mathbf{t}_i] = \sum_{i=1}^{N-1} \kappa_{i,i+1} (1 - \mathbf{t}_i \cdot \mathbf{t}_{i+1}) - J \sum_{i=1}^{N-1} \sigma_i \sigma_{i+1} - \mu \sum_{i=1}^N \sigma_i. \quad (1)$$

The angle $\gamma_{i,j}$ between two tangent vectors is given by $\cos \gamma_{i,j} = \mathbf{t}_i \cdot \mathbf{t}_j = \sin(\theta_i) \sin(\theta_j) \cos(\phi_i - \phi_j) + \cos(\theta_i) \cos(\theta_j)$. Equation (1) contains the dimensionless parameters $\kappa_{i,i+1} \equiv \beta \tilde{\kappa}_{i,i+1}$, $J \equiv \beta \tilde{J}$, and $\mu \equiv \beta \tilde{\mu}$. The first term in H is the bending energy of a discrete worm-like chain (DWLC) with a local dimensionless rigidity $\kappa_{i,i+1}$ that depends on the neighboring values of the Ising variables. The last terms make up the usual energy of the Ising model. The second term gives the energy $(2\tilde{J})$ of a domain wall (where σ_i passes from one value to another). The third term in μ (the chemical potential) gives the energy $(2\tilde{\mu})$ required to create a link in the state -1 (B link). The local rigidity is $\kappa_{i,i+1} = \kappa_A$ for a nearest neighbor link of type A-A, κ_B for B-B and κ_{AB} for A-B or B-A. In terms of the Ising field, $\kappa_{i,i+1} = \kappa_1 \sigma_i \sigma_{i+1} + \kappa_2 (\sigma_i + \sigma_{i+1}) + \kappa_3$ where $\kappa_1 \equiv (\kappa_A + \kappa_B - 2\kappa_{AB})/4$, $\kappa_2 \equiv (\kappa_A - \kappa_B)/4$, and $\kappa_3 \equiv (\kappa_A + \kappa_B + 2\kappa_{AB})/4$. We identify the B state with two identical non-interacting strands of ssDNA, each with a local rigidity equal to $\kappa_B/2$.

When all the bending rigidities are equal, the system decouples into a pure Ising model and a pure DWLC model (isomorphic to a 1D classical Heisenberg model for magnetism). The quantities that we will use to study the behavior of the coupled system are the mean “magnetization”, $c \equiv N^{-1} \sum_{i=1}^N \sigma_i$, the correlation functions for the Ising variables, $\langle \sigma_i \sigma_{i+r} \rangle$, and the chain tangent vectors, $\langle \mathbf{t}_i \cdot \mathbf{t}_{i+r} \rangle$, and the mean square end-to-end radius $R \equiv \langle \mathbf{R}^2 \rangle^{1/2}$. These correlation functions measure the extent of cooperativity exhibited by the coupled system: e.g., the size of the B (A) domains below (above) the melting temperature, and the length scale on which the chain remains rigid. The concentration of A and B links is given by $\varphi_A = (1 + \langle c \rangle)/2$ and $\varphi_B = 1 - \varphi_A$, respectively. The melting temperature $T_m < \infty$, if it exists, will be defined by $\varphi_A(T_m) = \varphi_B(T_m) = 1/2$. The partition and correlation functions for the coupled system can be calculated using transfer kernel techniques. For example, the partition function can be written as

$$Z = \sum_{\{\sigma_i = \pm 1\}} \prod_{i=1}^N \int \frac{d\Omega_i}{4\pi} \langle V | \sigma_1 \rangle \langle \sigma_1 | \hat{P}(\Omega_1, \Omega_2) | \sigma_2 \rangle \cdots \langle \sigma_{N-1} | \hat{P}(\Omega_{N-1}, \Omega_N) | \sigma_N \rangle \langle \sigma_N | V \rangle, \quad (2)$$

where the transfer kernel, which appears $N - 1$ times in Eq. (2), is given by

$$\hat{P}(\Omega_i, \Omega_{i+1}) = \begin{pmatrix} e^{\kappa_A [\cos(\gamma_{i,i+1}) - 1] + J + \mu} & e^{\kappa_{AB} [\cos(\gamma_{i,i+1}) - 1] - J} \\ e^{\kappa_{AB} [\cos(\gamma_{i,i+1}) - 1] - J} & e^{\kappa_B [\cos(\gamma_{i,i+1}) - 1] + J - \mu} \end{pmatrix} \quad (3)$$

with $|V\rangle = (e^{\mu/2}, e^{-\mu/2})$ the end vector, which enters in order to take care of the free chain boundary conditions. The A and B states form the canonical base, $|A\rangle = |+1\rangle = (1, 0)$ and $|B\rangle = |-1\rangle = (0, 1)$. Before presenting the full transfer kernel method, we first show that the partition function and averages of any quantities depending only on the Ising variables can be obtained by examining the effective Ising model obtained by integrating over the chain conformational degrees of freedom in Eq. (2). The problem reduces to that of an effective Ising model with an “effective free energy” $\beta H_{I,\text{eff}}^{(0)}$ containing renormalized parameters. This method works because, for the coupled Ising-chain system, the rotational symmetry is not broken. Hence the effective Ising transfer matrix, obtained by integrating the kernel $\hat{P}(\Omega_i, \Omega_{i+1})$

in Eq. (2) over Ω_i , is the same for any site:

$$\hat{P}_{I,\text{eff}}^{(0)} = \int \frac{d\Omega_i}{4\pi} \hat{P}(\Omega_i, \Omega_{i+1}) = e^{-\Gamma_0} \begin{pmatrix} e^{\mu_0 + J_0} & e^{-J_0} \\ e^{-J_0} & e^{-\mu_0 + J_0} \end{pmatrix} \quad (4)$$

where $J_0 \equiv J - [G_0(\kappa_A) + G_0(\kappa_B) - 2G_0(\kappa_{AB})]/4$ and $\mu_0 \equiv \mu - [G_0(\kappa_A) - G_0(\kappa_B)]/2 \equiv \mu - \Delta G_0^{AB}/2$ are the renormalized Ising parameters, and $\Gamma_0 \equiv [G_0(\kappa_A) + G_0(\kappa_B) + 2G_0(\kappa_{AB})]/4$. These parameters depend on chain rigidities through $G_0(\kappa)$ which is the (dimensionless) free energy of a single joint subsystem with rigidity κ : $G_0(\kappa) = -\ln\{\int \frac{d\Omega}{4\pi} \exp[\kappa(\cos(\theta) - 1)]\} = \kappa - \ln[\sinh(\kappa)/\kappa]$, an increasing function, varying as κ for $\kappa \ll 1$ and as $\ln(2\kappa)$ for $\kappa \gg 1$. The full partition function, $Z = Z_{I,\text{eff}}^{(0)} = e^{-(N-1)\Gamma_0} \sum_{\{\sigma_i\}} e^{-\beta H_{I,\text{eff}}^{(0)}[\sigma_i]}$, can be rewritten in terms of an effective Ising free energy:

$$\beta H_{I,\text{eff}}^{(0)} = -J_0 \sum_{i=1}^{N-1} \sigma_{i+1}\sigma_i - \frac{1}{2}\mu_0 \sum_{i=1}^{N-1} (\sigma_i + \sigma_{i+1}) - \frac{1}{2}\mu(\sigma_1 + \sigma_N). \quad (5)$$

Equation (5) shows that the free energy necessary to create a B link from an A one is $2\mu_0 \equiv 2\mu - \Delta G_0^{AB}$ for an interior link and $\mu + \mu_0 \equiv 2\mu - \Delta G_0^{AB}/2$ for an end link. The end links therefore have a tendency to remain in the A state. Although this end-interior asymmetry plays no role in the limit $N \rightarrow \infty$, it will play an essential role in determining how T_m varies with N . If the gain in the one link bending free energy in going from A to B, ΔG_0^{AB} , is greater than the intrinsic energy, 2μ , needed to break a closed bond, then the effective interior link chemical potential μ_0 becomes negative, signaling a change in stability of the A and B states.

The effective Ising partition and correlation functions can be obtained using Ising transfer matrix techniques [15]. We need the eigenvectors, $|0, \pm\rangle$, and the eigenvalues, $\lambda_{0,\pm}$ of the transfer matrix $P_{I,\text{eff}}^{(0)}$: $\lambda_{0,\pm} = e^{J_0 - \Gamma_0} [\cosh(\mu_0) \pm (\sinh^2(\mu_0) + e^{-4J_0})^{1/2}]$. We define the (dimensionless) free energy per Ising spin of the coupled system, $F = -N^{-1} \ln Z_{I,\text{eff}}^{(0)}$. The average Ising “magnetization” is obtained using $\langle c \rangle = -\partial F / \partial \mu$, from which φ_A and φ_B can be derived. The expression for $\langle c \rangle$ simplifies in the limit $N \rightarrow \infty$, because only the largest of the eigenvalues, $\lambda_{0,+}$, entering the effective Ising partition function survives:

$$\langle c \rangle \xrightarrow{N \rightarrow \infty} \langle c \rangle_\infty \equiv \frac{\partial f}{\partial \mu} = \frac{\sinh(\mu_0)}{[\sinh^2(\mu_0) + e^{-4J_0}]^{1/2}} \quad (6)$$

where $f = \lim_{N \rightarrow \infty} F = \lambda_{0,+}$. If μ_0 vanishes at a temperature, T_m^∞ , sufficiently low for the e^{-4J_0} term in the denominator to be small, then the system will undergo a sharp melting transition: $\langle c \rangle_\infty$ will sharply cross-over from +1 for $T < T_m^\infty$ (pure A state) to -1 for $T > T_m^\infty$ (pure B state). Contrary to previous Ising-type models, the melting temperature is not put in by hand but emerges naturally from $\mu_0 = 0$. The size of the e^{-4J_0} term in Eq.(6) will determine the width of the transition region, $\Delta T_m^\infty \equiv 2|\partial \langle c \rangle_\infty / \partial T|_{T_m^\infty}^{-1} \approx (2k_B T_m^2 / \tilde{\mu}) \exp[-2J_0(T_m)]$. In the double limit $N, i \rightarrow \infty$, we ignore the influence of end-monomers and the Ising correlation function reduces to the simpler cyclic boundary condition form, $\langle (\sigma_i - \langle c \rangle_\infty)(\sigma_{i+r} - \langle c \rangle_\infty) \rangle \rightarrow (1 - \langle c \rangle_\infty^2) \exp(-r/\xi_I)$, where we have introduced the Ising correlation length, $\xi_I = -\ln^{-1}(\lambda_{0,-}/\lambda_{0,+})$. Because the system is translationally invariant in this limit, the Ising correlation length measures the range of correlations between spatially separated deviations of the local Ising spin from the average value (see Fig. 1b).

Full transfer kernel approach. – To calculate the general chain tangent-tangent correlation function, $\langle \mathbf{t}_i \cdot \mathbf{t}_{i+r} \rangle$, for the coupled model, we need to introduce the more powerful

(but more abstract) transfer kernel method [16]. This method will also shed additional light on the origin of the effective Ising model obtained above by first integrating out the chain degrees of freedom. To calculate the partition and correlation functions using this method, we need to solve a spinor eigenvalue problem: $\hat{P}|\hat{\Psi}\rangle = \lambda|\hat{\Psi}\rangle$, where $|\hat{\Psi}(\Omega)\rangle = (\Psi_{+1}(\Omega), \Psi_{-1}(\Omega))$. We find eigenvalues, $\lambda_{l,\tau}$, labeled by $l = 0, \dots, \infty$ and $\tau = \pm$ with the same form as for $l = 0$ given above but now where G_0 in the renormalized parameters is replaced by $G_l(\kappa) = \kappa - \ln[\kappa^l(d/\kappa d\kappa)^l(\sinh(\kappa)/\kappa)]$ [17]. The eigenspinors are $|\hat{\Psi}_{l,m;\tau}(\Omega)\rangle = \sqrt{4\pi}Y_{lm}(\Omega)|l, \tau\rangle$ where $Y_{lm}(\Omega)$ are the spherical harmonics. The transfer kernel can be expanded in terms of the eigenspinors $\hat{P} = \sum_{l,m,\tau} \lambda_{l,\tau} |\hat{\Psi}_{l,m;\tau}\rangle \langle \hat{\Psi}_{l,m;\tau}|$ and by inserting it in Eq. (2), we find the same result obtained by solving the effective Ising model defined by Eq. (5):

$$Z = \langle V | \hat{P}^{N-1} | V \rangle = \sum_{l,m;\tau} \langle V | \hat{\Psi}_{l,m;\tau} \rangle^2 \lambda_{l,\tau}^{N-1} = \sum_{\tau=\pm} \langle V | 0, \tau \rangle^2 \lambda_{0,\tau}^{N-1} = Z_{1,\text{eff}}^{(0)} \quad (7)$$

where we have used $\langle \hat{\Psi}_{l,m;\tau} | V \rangle = \delta_{l0}\delta_{m0}\langle 0, \tau | V \rangle$. These eigenspinors and their corresponding eigenvalues can be simplified in two important limits: (i) For sufficiently low temperatures, above or below any possible transition temperature, T_l^∞ (at which μ_l vanishes), the inequality $\sinh|\mu_l| \gg e^{-2J_l}$ is obeyed. Taking the $l = 0$ case as an example, the off-diagonal (domain-wall) terms in Eq. (4) can be neglected and the eigenvectors reduce asymptotically to the canonical ones; this mapping holds for all l and depends on the sign of μ_l : $|l, +\rangle \approx |A\rangle$ and $|l, -\rangle \approx |B\rangle$ if $\mu_l > 0$ and $|l, -\rangle \approx |A\rangle$ and $|l, +\rangle \approx |B\rangle$ if $\mu_l < 0$. (ii) For temperatures at or very near the transition temperature, the opposite inequality $\sinh|\mu_l| \ll e^{-2J_l}$ holds and μ_l can be set to zero: the eigenvectors then reduce to symmetric and anti-symmetric superpositions of the canonical basis vectors: $|l, \pm\rangle \approx (|A\rangle \pm |B\rangle)/\sqrt{2}$.

In the double limit $N, i \rightarrow \infty$, the dependence on the chain ends disappears, the expression for the tangent-tangent correlation function simplifies to

$$\langle \mathbf{t}_i \cdot \mathbf{t}_{i+r} \rangle \underset{N, i \rightarrow \infty}{\rightarrow} \sum_{\tau} \langle 1, \tau | 0, + \rangle^2 \exp[-r/\xi_{1,\tau}^p] \quad (8)$$

which reveals the importance of the two persistence lengths, $\xi_{1,\pm}^p = -\ln^{-1}(\lambda_{1,\pm}/\lambda_{0,+})$, and the two “transition probabilities”, $\langle 1, \pm | 0, + \rangle^2$, for going from the “ground state” $|0, +\rangle$ to the “first excited states”, $|1, \pm\rangle$. The relevance of both $\xi_{1,\pm}^p$ and the associated weights is discussed below with standard parameter values for dsDNA and ssDNA.

Application to synthetic DNA thermal denaturation. – Melting or thermal denaturation profiles, $\varphi_B(T)$, are experimentally obtained by following the UV absorbance of a DNA solution while slowly increasing the sample temperature. A typical profile has a sigmoid shape possibly with bumps depending on the DNA sequence. In this section, we compare the model developed above with experiment [4]. We focus on the evolution of $\varphi_B(T)$ for a synthetic homopolynucleotide polydA-polydT. Five independent parameters appear in the theory: the polymerization index N , Ising parameters μ and J , and bending modulii κ_A for dsDNA and κ_B for ssDNA (without any loss of generality, we choose to fix $\kappa_{AB} = \kappa_A$, see [16] for details).

Figure 1a shows $\varphi_B(T)$ for a polydA-polydT of molecular weight $M_w = 1180$ kda ($N = 1815$) in a solution of 0.1 SSC [4]. In order to compare the data with our model predictions, we choose for the known persistence lengths the experimental values $\ell_A^p = 50$ nm and $\ell_B^p = 1$ nm, which lead to $\kappa_A = 147$ and $\kappa_B = 5.54$ at room temperature (using $a = 0.34$ nm for base-pair size and a factor of 2 for two parallel flexible segments per coil). The length $N = 1815$ is given. By setting the melting temperature T_m equal to 326.4 K, the two remaining parameters μ and J are in fact related, leaving only *one free parameter*. The solid line in Fig. 1a corresponds to

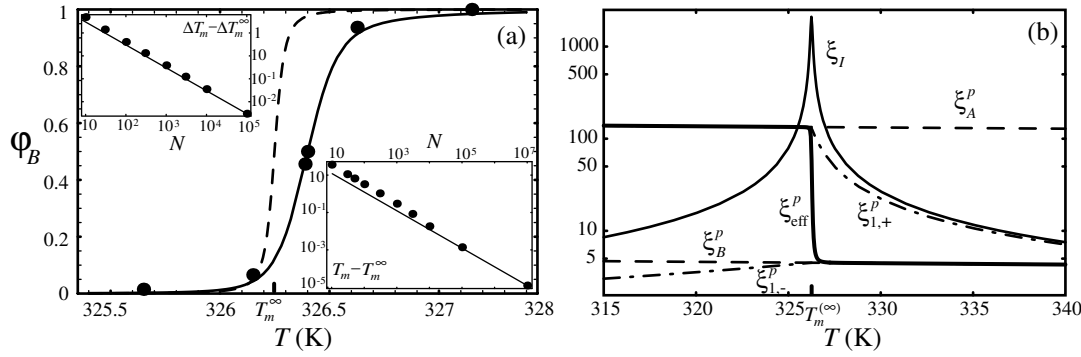


Fig. 1 – (a) Fraction of broken base-pairs *vs.* temperature for polydA-polydT (data for 0.1 SSC, $N = 1815$ [4]). The solid line represents the theoretical result for $\mu = 1.64 k_B T_m$ and $J = 3.35 k_B T_m$ where $T_m = 326.4$ K. The broken line corresponds to $N \rightarrow \infty$ (same parameter values). Insets: Model results for the shift of the melting temperature $T_m - T_m^\infty$ and the transition width $\Delta T_m - \Delta T_m^\infty$ *vs.* polymer length. (b) Ising correlation length, ξ_I , persistence lengths of the coupled system, $\xi_{A,B}^p = R^2/(2a^2 N)$, $\xi_{1,\pm}^p$, and of pure chains, $\xi_{1,\pm}^p$ (in units of a) *vs.* temperature. At T_m^∞ , the effective persistence length, ξ_{eff}^p , jumps from $\xi_{1,+}^p \approx \xi_A^p = \ell_A^p/a \approx 147$ to $\xi_{1,-}^p \approx \xi_B^p = 2\ell_B^p/a \approx 5$.

$\mu = 1.64 k_B T_m \simeq 4.46$ kJ/mol and $J = 3.35 k_B T_m \simeq 9.13$ kJ/mol. We can then deduce several thermodynamical features. Noting that the chemical potential for creating one A-T link is, in our model, 2μ , we find a value very close to the experimental one of 10.5 kJ/mol [2]. Although the value of J is more difficult to interpret, it is related to the stacking energy which is lost by unstacking two consecutive bases. Our result $J \sim 2\mu$ is consistent with the idea that stacking interactions make the dominant contribution to DNA stability [3]. Chain fluctuations do not only renormalize the bare chemical potential, μ but also the bare cooperativity parameter J : J_0 varies with T contrary to previous theories [6] where J was taken as constant and supposed to be purely entropic in character. We have for the total cooperativity parameter $J_0 = 4.17 k_B T_m$ at $T = T_m$, which shows that the bending contribution is roughly 25%. The model thus leads to parameter values comparable with experimental data.

In Fig. 1a, the curve corresponding to the thermodynamic limit ($N \rightarrow \infty$) is shown for the same parameter values. In this case, $\varphi_B(T)$ is given by Eq. (6) and the value of μ is obtained as a function of T_m using $\mu_0(T_m) = 0$: $2\tilde{\mu} = k_B T_m \Delta G_0^{AB} \simeq k_B T_m \ln(\tilde{\kappa}_A/\tilde{\kappa}_B)$, valid at melting temperature. Hence, the melting temperature is reached when the chemical potential required to create a link is perfectly balanced by the difference in free energy of the two types of semi-flexible chains. Contrary to previous models, where two fitting parameters, related to μ and J , are used once T_m is inserted, here the experimental knowledge of dsDNA and ssDNA persistence lengths reduces them to one. Another quantity which has an experimental relevance is the width of the transition. In the thermodynamic limit, this width is non-zero, due to the cooperativity parameter: $\Delta T_m^\infty \sim \exp[-2J_0(T_m)] \sim \xi_I^{-1}(T_m)$. When N decreases, the width increases as plotted in Fig. 1a. It roughly follows the law $\Delta T_m(N) - \Delta T_m^\infty \sim N^{-1}$. One observes that even for a long polymer ($N \sim 10^3$) finite size effects are non-negligible. For $N \sim 10$, we predict a large transition width of 50 K. This point is crucial since it has been observed experimentally that melting curves are much wider for very short DNA chains (around 10 bp) [18]. In such experiments, the nature of end monomers becomes important. By focusing on finite-size effects, Fig. 1a shows that $T_m(N)$ increases when N decreases, following a law in $1/N$. Moreover the shape of the $\varphi_B(T)$ curve becomes less and less symmetrical when

N decreases [16]. Such an asymmetry contrasts with what was observed in previous models [6], where the sigmoidal shape is always symmetrical (both for finite N and $N \rightarrow \infty$) unless the end monomers states are given. In our model, the bending contribution for end monomers is half of an interior monomer one, which breaks this symmetry even for free boundary conditions, as seen in Eq. (5). This is corroborated by experimental measurements [6].

Included in the predictions of our theory are mechanical and structural features of the composed chain, such as persistence length or mean square radius, R . This contrasts with purely Ising-type models where only thermodynamical quantities related to base-pairing are available. The calculation of tangent-tangent correlation functions, Eq. (8), reveals two characteristic lengths (in units of a), $\xi_{1,\pm}^p$. Hence, it is not possible to extract from Eq. (8) one unique length for the whole range of T , as usually done for semi-flexible chains. From the expression for R in the limit $N \rightarrow \infty$, we can, however, define an effective persistence length: $R^2 \simeq 2a^2 N \xi_{\text{eff}}^p = 2a^2 N \sum_{\tau} \langle 1, \tau | 0, + \rangle^2 \xi_{1,\tau}^p$. Due to the coupling between bending and internal states, the respective weights $\langle 0, + | 1, \pm \rangle^2$ associated with each correlation length change abruptly at T_m : below T_m , we have $\langle 0, + | 1, + \rangle \approx \langle A | A \rangle = 1$ and $\langle 0, + | 1, - \rangle \approx \langle A | B \rangle = 0$ and thus $\xi_{\text{eff}} \approx \xi_{1,+}^p \approx \xi_A^p$; whereas above T_m , we find $\langle 0, + | 1, + \rangle \approx \langle B | A \rangle = 0$ and $\langle 0, + | 1, - \rangle \approx \langle B | B \rangle = 1$ which yields $\xi_{\text{eff}} \approx \xi_{1,-}^p \approx \xi_B^p$. Variation of this effective persistence length is shown in Fig. 1b. Since the transition is very abrupt, we suggest that the denaturation transition can also be observed experimentally by measuring directly the radius of gyration, for instance by light-scattering, viscosity or tethered particle motion experiments.

The foregoing analysis makes no allowance for solvent entropic (hydrophobic) and electrostatic effects which might change the actual energy values of base-pair formation and a domain wall. To go further concerning solvent entropic effects would require molecular dynamics simulations and is beyond the scope of the present approach. Electrostatic effects in DNA melting have an entropic contribution due to counterion release [19]. At equilibrium, this contribution is roughly on the same order of magnitude as the one coming from chain fluctuations and should be included in a more refined model [16].

REFERENCES

- [1] SANTALUCIA JR. J., *Proc. Nat. Acad. Sci. USA*, **95** (1998) 1460.
- [2] PINCET P. ET AL., *Phys. Rev. Lett.*, **73** (1994) 2780.
- [3] GOTOH O., *Adv. Biophys.*, **16** (1983) 1.
- [4] WARTELL R.M. and MONTROLL E.W., *Adv. Chem. Phys.*, **22** (1972) 129.
- [5] KALOSAKAS G. ET AL., *Europhys. Lett.*, **68** (2004) 127.
- [6] NELSON P., *Biological Physics*. (W.H. Freeman and Co., New York) 2004, sect. 9.
- [7] FICHE J.B. ET AL., *Biophys. J.*, (2006) doi:10.1529/biophysj.106.097790.
- [8] YAN J. and MARKO J.F., *Phys. Rev. Lett.*, **93** (2004) 108108.
- [9] SMITH S.B., FINZI L. and BUSTAMANTE C., *Science*, **258** (1992) 1122.
- [10] POUGET N. ET AL., *Nucleic Acids Res.*, **32** (2004) e73.
- [11] WIGGINS P.A. ET AL., *Nature Nanotechnology*, **1** (2006) 137.
- [12] PEYRARD M. and BISHOP A.R., *Phys. Rev. Lett.*, **62** (1989) 2755.
- [13] PALMERI J. and LEIBLER S., *Dynamical Phenomena at Interfaces, Surfaces and Membranes*, edited by D. BEYSENS, N. BOCCARA and G. FORGACS (Nova Science, Inc., New York) 1993.
- [14] STORM C. and NELSON P.C., *Europhys. Lett.*, **62** (2003) 760.
- [15] MCCOY B. and WU T.T., *The two Dimensional Ising Model* (HUP, Cambridge, MA) 1973.
- [16] PALMERI J., MANGHI M. and DESTAINVILLE N., *in preparation*, (2007) .
- [17] JOYCE G.S., *Phys. Rev.*, **155** (1967) 478.
- [18] ALTAN-BONNET G., LIBCHABER A. and KRICHEVSKY O., *Phys. Rev. Lett.*, **90** (2003) 138101.
- [19] KOROLEV N. and LYUBARTSEV A.P. and NORDENSKILD L., *Biophys. J.*, **75** (1998) 3041.